/ 49

Field-dependent critical currents in thin Nb superconducting disks

J. Zhu[1], James Lockhart[2,3], John Turneaure[2]

[1]Read-Rite Corporation, 345 Los Coches Street, Milpitas, CA 95035, U.S.A.
[2]Hansen Experimental Physics Laboratory, Stanford University, Stanford, CA 94305, U.S.A.
[3]Physics Department, San Francisco State University, San Francisco, CA 94132, U.S.A.

Keywords: superconductor, critical state model, thin film, Nb, hysteresis loop

Abstract

Magnetic hysteresis loops were measured on thin Nb superconducting disks using a SQUID-based technique; field-dependent critical currents have been observed in thin superconducting disks at low magnetic flux trapping densities ($\leq$4G). Such phenomena were found to exist over a wide range of temperatures below the transition temperature. The observed field-dependent critical current densities are attributed to long range interactions between trapped vortices in a superconducting film whose thickness is much less than or comparable to the penetration depth. In the framework of Kim's critical state model, we developed a numerical method to calculate the field-dependent critical currents by fitting the measured magnetic hysteresis loop. Our experimental data were adequately explained by Kim's critical state model. Shielding currents and magnetic field patterns in thin superconducting disks were calculated.

1 Introduction

Recently there has been increasing interest in non-destructive measurements of thin film critical parameters [1, 2, 3] of type-II superconductors. Disk-shaped type-II superconductors have been treated [1, 2, 4] in the framework of the critical state model[5] with magnetic fields applied perpendicular to the film plane. Analytical solutions assuming a constant critical current have been found for current and field patterns in disk-shaped type-II superconductors [1, 6]. Constant critical currents are often assumed to calculate shielding current and magnetic field patterns for the sake of simplicity.

In a bulk type-II superconductor, the supercurrent of a trapped vortex decreases exponentially with large distance ($r \gg \lambda$, where λ is the penetration depth); therefore the interactions between trapped magnetic vortices are important only when trapped vortices are separated by distances comparable to or less than the penetration depth($r \sim \lambda$). However, for a type-II thin film superconductor whose thickness d is much less than or comparable to the penetration depth λ, the screening capacity for a trapped vortex is weak; as a result, the supercurrent of the trapped magnetic vortex is more spread out than for the case of a long vortex line. In fact the current density $j(r)$ decays as [7]

$$j(r) \sim 1/r, \text{ for } \xi \ll r \ll \lambda^2/d$$

$$j(r) \sim 1/r^2, \text{ for } r \gg \lambda^2/d$$

in a thin film, where ξ is the coherence length of the superconductor. Since $j(r)$ decays very slowly with distance r, interactions among trapped vortices are important even at low flux trapping densities; thus we predict field-dependent critical currents at low flux densities in thin films. Experiments were carried out to measure such field-dependent critical currents.

From the experimental standpoint, magnetization measurements are the most widely used contactless method to measure the critical current density. Magnetization measurements are often performed on a slab or cylindrical sample where the demagnetization factor is negligible along the external magnetic field direction; however, for a thin plate sample with magnetic field applied normal to the film plane, or the z-direction, the demagnetization effect becomes dominant in that direction; hence one must be particularly cautious when calculating the critical current for the above case [4]. For field-dependent critical current models, a finite element analysis method has to be employed to calculate the critical states in disk-shaped type-II thin film superconductors.

In this paper, we report observations of field-dependent critical currents in disk-shaped Nb thin films. Using a SQUID-based technique, we measured magnetic hysteresis loops on several Nb samples. Field-dependent critical currents were observed in all cases over a wide range of temperatures below the transition temperature. In the framework of the critical state model, we developed a numerical method to obtain field-dependent critical currents by fitting the measured magnetic hysteresis loops. The Kim type critical current model was used in our calculation. We also calculate shielding current and magnetic field patterns in disk-shaped Nb films.

2 Experiment

The disk-shaped thin film Nb samples were dc-sputtered onto a quartz substrate through a shadow mask as listed in Table 1. RRR is the residual resistance ratio defined as R(300K)/R(10K).

Table 1: **Dc-sputtered Nb samples**

sample	thickness (Å)	T_c (K)	RRR	diameter (cm)
Sample #2	1350	8.57	2.5	0.848
Sample #4	2500	8.76	2.8	0.734
Sample #5	1750	8.79	3.0	0.927

Fig. 1 shows the experiment setup. A superconducting pickup loop coupled to a SQUID was used to measure magnetic hysteresis in the sample. The pickup loop is a thin film circular Nb track of radius $0.25cm$ printed on a sapphire substrate. The pickup loop is placed concentric with, parallel to and $0.20mm$ above the sample; therefore, it is only sensitive to the z component of magnetic fields and to the area of the sample that is directly below the pickup loop. The sample is placed in the center of a solenoid which generates external magnetic fields normal to the sample plane. The sample and pickup loop are enclosed in a vacuum housing; the SQUID is enclosed in another vacuum housing. A superconducting vacuum feedthrough is used to connect the pickup loop to the SQUID. The pickup loop substrate is thermally anchored to the liquid Helium bath; while thermal isolation is provided between the sample and the bath. A total power of $3mW$ is needed to heat the sample from 4.2K to 12K; and it takes about three minutes for samples to cool back to 4.2K after the heaters are turned off.

The sample is zero-field-cooled (ZFC) or field-cooled (FC). The initial trapped field in the sample is always assumed to be uniform. The initial dc field (FC) was kept on all the time during the measurements. An ac magnetic field was applied to measure the magnetic hysteresis loops at low frequencies ($\leq$ 1mHz) so as to minimize the flux creeping effect. The measurements were terminated after the equilibrium magnetic hysteresis loop was reached. Only weak applied magnetic fields were used in our experiments; the average distance between any two neighbor vortices was kept much larger than the penetration depth λ of the superconductor. Direct coupling between the pickup loop and the external field was nulled to better than 2 parts in 10^4 by feeding a proportional current back to the SQUID input loop.

Fig. 2 shows examples of magnetic hysteresis loops measured on sample #4 at 8.56K. In the left half of Fig. 2 the sample was FC in a field of +0.5 Oe, where the positive sign represents the $+z$ direction; in the right half of Fig.2 the sample was FC in a field of -0.5 Oe. An ac field of $0.5\sin(2\pi ft)$ Oe was applied to measure the hysteresis loops, where $f = 10^{-3}$Hz. First we argue that the critical current is field-dependent in the above experiments. If the critical current had been field-independent, the experimental hysteresis loops would also have been field-independent; however, in Fig. 2 the magnetic hysteresis loops were shifted in the direction of the initial dc field; therefore the critical current was dependent of the trapped flux density. Second we argue that the critical current decreases with increasing flux trapping density; the shift of hysteresis loops in the direction of the initial trapped dc field indicated that magnetic fields penetrated more easily into the superconducting sample in the direction of the initial dc field than in the opposite direction; so the critical current density was lower for higher flux density. We have thus observed field-dependent critical current densities in superconducting Nb thin films, which decreases with increasing flux density.

Fig. 3 shows the magnetic hysteresis loop measured on sample #2 at 7.89K, well below its transition temperature $T_c = 8.57$K. In the left half of Fig. 3 the sample was ZFC; in the right half of Fig. 3 the sample was FC in a field of +2.4 Oe. An ac field of $-1.2\sin(2\pi ft)$ Oe was applied to measure the hysteresis loops, where $f = 10^{-3}$Hz and the negative sign represents the initial condition of the ac field. Although the measurements were performed at a temperature well below the transition temperature and at low flux densities, significant suppression of the critical current was apparent in the FC experiment in Fig. 3. We estimate the penetration depth λ at 7.89K to be about 770Å using the penetration depth λ(0K)=410($\pm$10)Å of pure bulk Nb [8] and the relation, $\lambda(\mathrm{T})=\lambda(0\mathrm{K})/\sqrt{1-(T/T_c)^4}$. Impurities in the sample increase the penetration depth λ somewhat. We conclude that the penetration depth λ(7.89K) of the sample #2 is on the order of its thickness (d = 1350Å). The maximum flux density in the experiment was estimated to be less than 4.0 G. The average distance between any two trapped vortices was thus larger than 2.3μm, which was about 30 times larger than the penetration depth λ(7.89K) of pure bulk Nb. The observed reduction in the critical current in Fig. 3 at such low flux densities can be attributed to the long range interactions between trapped vortices due to slow radial fall-off of supercurrents of trapped vortices in thin film superconductors.

3 The Critical State Model

3.1 Field-Dependent Critical Current Density

In this section, we show that interactions between flux lines are of short range in a bulk superconductor. We also show that interactions between vortices are long range in a thin film superconductor whose thickness is comparable to or less than the penetration depth.

In a bulk superconductor, the interaction energy between vortex lines is given by [7]

$$U_{12}^{bulk} = \frac{\Phi_o^2}{8\pi^2\lambda^2}\sqrt{\frac{\pi\lambda}{2r_{12}}}e^{-\frac{r_{12}}{\lambda}}, \quad \text{for } r_{12} \gg \lambda, \tag{1}$$

where U_{12}^{bulk} represents the repulsion interaction energy per unit length of two vortex lines; r_{12} is the distance between the two vortex lines in a bulk superconductor; and Φ_o is the flux quantum. The expulsion force can be computed by taking derivatives of the interaction energy U_{12}, that is, $\vec{f}_{12} = -\nabla U_{12}$. Eqn. (1) indicates that interactions between vortex lines are important only when the distance between vortex lines is comparable to or less than the penetration depth.

In a thin film superconductor, assuming constant current densities in the thickness, the interaction energy between two vortex vortices is given by [7]

$$U_{12}^{film} = \frac{\Phi_o^2}{4\pi^2 d r_{12}}, \quad \text{for } r_{12} \gg \lambda^2/d, \tag{2}$$

where U_{12}^{film} represents the repulsion interaction energy per unit length of two vortex lines in a thin film superconductor, and d is sample thickness. Eqn. (2) indicates that the expulsion force between vortex vortices is long range in a thin film ($d <\sim \lambda$) [7], since the expulsion force f_{12} decays as $1/r^2$ for $r \gg \lambda^2/d$. This long range is due to the fact that most of the interaction takes place not through the superconductor, but through the empty space above and below the film. Since long range interactions prevent trapped vortices from acting independently, field-dependent critical currents are expected in thin superconducting disks at low flux densities where the distance between vortices is much larger than the penetration depth.

Bean [5] first explained some of the features of a hysteric superconductor assuming $j_c = \text{const}$. Kim, Hempstead, and Strnad [9] used the critical state equation

$$j_c(B) = \frac{\alpha}{B + B_o} \tag{3}$$

to discuss the magnetization of hollow superconducting cylinders, where α and B_o are material-dependent constants. Eqn. (3) is also used in our numerical model to approximate the relationship between the critical current density and the trapped flux density.

3.2 Finite Element Analysis

Frankel [10] and Däumling and Larbalestier [4] employed numerical methods to solve the critical state equation in disk-shaped superconductors for Bean type and Kim type critical currents. Using the finite-element analysis, Frankel [10] applied the critical state model to calculate the magnetic field and the current distribution numerically for superconducting disks in transverse fields. Däumling and Larbalestier [4] extended their calculations further to disks with different aspect ratios. The applicability of the critical state model in a disk sample has been discussed extensively by Däumling and Larbalestier [4] and also by Conner and Malozemoff [11].

In our model, we also use the finite element analysis. The thin superconducting disk is divided into N_s equally spaced concentric loops. The circulating current density is assumed to be uniform in the thickness, which is a good approximation for disk thickness $d \leq 2\lambda$. Calculations are carried out in cylindrical coordinates, with a magnetic field H_{appl} applied in the z direction. Shielding currents only flow in the azimuthal direction because of the symmetry of the sample. Consider a superconducting loop (l_m) which encloses a number of N_m of flux quanta. Flux quantization gives

$$\Phi_m + \frac{4\pi\lambda^2}{c} \oint d\mathbf{lm} \cdot \mathbf{jm} = N_m \Phi_o, \tag{4}$$

where Φ_m is the total flux in the loop; integrals $\oint d\mathbf{lm}$ are taken along the loop l_m; and j_m is the current density. The disk is treated as a system of a number of N_s equally-spaced concentric superconducting loops, thus

The enclosed flux in each loop is

$$\Phi_i = \Phi_i^a + \frac{1}{c} \sum_{k=1}^{N_s} M_{ik} I_k, \tag{5}$$

where $i = 1, 2, ..., N_s$; and $\Phi_i^a = H_{appl} \pi R_i^2$, R_i is the radius of i-th loop, I_k is the total current flowing in k-th loop, Φ_i is the total flux enclosed by i-th loop, M_{ik} represents the mutual inductance between the i-th loop and the k-th loop, and M_{ii} is the self-inductance of the i-th loop. Combining Eqns. (4) and (5) gives us the following:

$$\Phi_i^a + \frac{1}{c} \sum_{k=1}^{N_s} M_{ik} I_k + \frac{4\pi\lambda^2}{c} \oint d\mathbf{l_i} \cdot \mathbf{j_i} = N_i \Phi_o, \tag{6}$$

under the constraint:

$$|j| \leq j_c(B_z), \tag{7}$$

here $i = 1, 2, ..., N_s$, and $j_i = I_i/wd$, where w is the loop width and d is the sample thickness; the critical current density $j_c(B_z)$ is a function of the averaged axial field B_z at radius R_i of the i-th loop; and N_i is the number of fluxons in the i-th loop.

The mutual inductance M_{ab} of two concentric loops l_a and l_b separated by a vertical distance z in a vacuum is

$$M_{ab} = \oint \oint \frac{d\mathbf{l_a}\, d\mathbf{l_b}}{R_{ab}}, \tag{8}$$

where the integrations are taken along the circular loops l_a and l_b; R_{ab} is the distance between element $d\mathbf{l_a}$ and $d\mathbf{l_b}$. Eqn. (8) assumes the loops have zero width. The integration of Eqn. (8) gives us [12]

$$M_{ab} = 4\pi\sqrt{r_a r_b}[(\frac{2}{s} - s)K(s) - \frac{2}{s}E(s)] \tag{9}$$

where $s^2 = 4r_a r_b/[(r_a + r_b)^2 + z^2]$, and $K(s)$ and $E(s)$ are complete elliptic integrals of the first and the second kinds; r_a and r_b are the radii of the two loops. The self-inductance of a circular loop M_{aa} is calculated as follows [13]

$$M_{aa} = 4\pi r_a(\log\frac{8r_a}{w} - 0.5), \tag{10}$$

where w is the width of the tape-like circular sample loop and the thickness of the sample is negligible comparing to the width of the tape. The kinetic inductance here is assumed to be negligible; the assumption is valid as long as the condition, $\lambda \ll \sqrt{wd}$, is satisfied, where w is the loop width and d is the film thickness.

The critical state Eqn. (6) can be solved by iteration once the form of $j_c(B_z)$ is known. We used the Kim relation $j_c = \alpha/(B + B_o)$ in our calculations. The solutions to Eqn. (6) are eventually used to calculate the total flux in the pickup loop which is then compared with our experimental results. We found that the solutions to the total flux in the pickup loop are nearly independent of N_s used for solving Eqn. (6) if the sample loop widths are less than several times the spacing distance between the pickup loop and the sample plane. A value of N_s of 100 is adequate for all our calculations.

An iteration method is employed to solve Eqns. (6) and (7). We start with either the ZFC or FC sample and apply an ac field. Shielding currents in the loops are first estimated assuming perfect shielding against the change of the external field. The estimated shielding currents are then compared with the Kim type critical current $I_c(B_z)$ calculated using the local flux density B_z. If the estimated i-th loop current I_i (density j_i) is larger than the critical current I_c^i (density j_c^i), the corresponding N_i has to be adjusted to $N_i \pm \delta N_i$, where the sign depends on the direction of the shielding current and δN_i is given by

$$\delta N_i = M_{ii}(I_i - I_c^i),$$

where M_{ii} is the self-inductance of the i-th sample loop. The above procedure is repeated until the critical current constraint is satisfied everywhere in the sample.

Penetrated flux density profiles or shielding current patterns are obtained iteratively by using the above method. The change of flux in the pick-up loop due to the magnetic field penetration into the sample can also be calculated. The magnetic hysteresis loop is calculated by cycling the sample in an ac field.

In the limit of a constant critical current density, the above numerical analysis gives the same solutions to the critical state equation as the analytic solutions presented in Ref.[6].

4 Results

Fig. 4 shows an example of calculated current and field patterns in sample #4. The sample was FC in a field of -0.5 Oe applied normal to the film. At state **A**, the value of the ac field was increased from zero to $+1.2$ Oe; the value of the ac field was then reversed to -1.2 Oe to reach state **B**; at state **C**, the value of the ac field was again increased back to $+1.2$ Oe. The field-dependent critical current density used in the calculation was Kim type: $j_c = 5.38 \times 10^4/(1 + 1.08|B_z|)A/cm^2$. First we note that shielding currents flow in the region of *uniformly* trapped vortices; second we note that state **C** is different from **A** due to initial field trapping and field-dependent critical currents, which was also observed experimentally; finally, no discontinuities were found in the shielding currents, as pointed out in Ref.[6], which is very different from the critical current patterns in a bulk superconductor.

Once penetrated flux density profiles or shielding current patterns were obtained, the flux density change in the pickup loop can be calculated, therefore the total flux change in the pickup loop can be determined. As the applied field is varied, hysteresis is expected because of the presence of pinning in type-II superconductors. Fig. 2 shows the experimental magnetic hysteresis loops observed on Nb sample #4 at temperature of 8.56K. Also shown are the theoretical magnetic hysteresis loops calculated using our finite element analysis. In the left half of Fig. 2, there is a striking similarity between the theoretical calculation and the measurement, especially the "crossing" point, where the initial magnetization curve clearly crossed the later magnetic hysteresis loops. In the right half of Fig. 2, the initial experimental magnetization curve is higher than the later equilibrium magnetic hysteresis loop; the theoretical calculation also showed the same characteristics: the magnetization of state **A** is clearly higher than that of state **C**. The agreement between the calculation and the measurement was acceptable considering the fact that the actual critical current may be much more complicated than the simple Kim critical state Eqn. (3).

The pickup loop measured the z-directed flux in the sample under the pickup loop. Fig. 5 shows the z-direction field at the pickup loop when the value of the ac field was maximum in the $+z$ direction and the $-z$ direction at 8.70K in sample #5. Each pair of points was extracted from a hysteresis loop measurement. For each measurement, the sample was heated above its transition temperature, and then FC in a dc magnetic field. The ac field was applied in addition to the dc field to measure the hysteresis loop. Since the dc fields were applied in the $-z$ direction, the magnetic hysteresis loops were enhanced in that direction. For comparison, we also show the simulation data using the Kim type critical current density $j_c = 7.2 \times 10^3/(1 + 0.22|B_z|)A/cm^2$. In the $-z$ direction, the simulation data showed a monotonic trend as the experiment data did; in the $+z$ direction the simulation results showed a dip as the experiment data did, although the dip is not as large as that of the experimental data. The overall agreement was considered very good between the measurements and the simulation results. For dc fields much larger than the ac field the simulation results showed a much better fit.

5 Discussion of Results

In Fig. 5, the critical current density decreases with increasing flux density. The assumption of constant critical currents at low flux density [14] in thin films is only an approximation; and the assumption is reasonable if the trapped flux density does not vary much across the sample.

In Fig. 5, Kim's critical state Eqn. (3) is a very good approximation for dc fields larger than 2.0 Oe; however, the theoretical calculations deviate from the experimental measurements for lower dc fields. The deviations indicate that the actual critical state equation is more complicated than the simple Kim's critical state equation 3 at low flux density in type-II thin film superconductors. More refined field-dependent critical current relations can certainly be introduced into our numerical method to obtain a better fit; however, there is no evidence that more physical insight into flux pinning and vortex interactions can be obtained in this manner.

Eqn. (2) revealed long range interactions between vortices in a type-II thin film whose thickness is comparable to or less than its penetration depth. Our experiments have shown field-dependent critical currents to confirm the important role played by vortex interactions in thin superconducting films.

In summary, we have observed field-dependent critical currents in thin Nb superconducting disks at low flux densities; and we attribute the dependence to the slow decrease of supercurrents of trapped vortex in thin superconducting films. In the framework of the critical state model, we developed a numerical method to calculate the field-dependent critical current density by fitting the magnetic hysteresis loop measured using a SQUID-based technique. Good agreement was obtained between the experimental results and our calculation using the Kim critical state model.

Acknowledgments

We would like to thank D. Gill for his help in preparing the Nb thin films. We also thank Professor J. R. Clem for helpful discussions and correspondence. This research was supported by NASA Contract NAS8-36125 from the George C. Marshall Space Flight Center.

References

[1] P.N. Mikheenko and Yu.E. Kuzovlev, Physica C 204 (1993), 229-236.

[2] H. Theuss, A. Forkl and H. Kronmüller, Physica C 190 (1992), 345.

[3] Y. Yokoyama, Y. Hasumi, H. Obara, Y. Suzuki, T. Katayama, S. Gotoh and N. Koshizuka, Jpn. J. Appl. Phys. 30 (1991), L714.

[4] M. Däumling and D. C. Larbalestier, Phys. Rev. B. **40**,9350(1989).

[5] C. P. Bean, Phys.rev. lett. **8**, 250(1962).

[6] J. Zhu, John Mester, James Lockhart, and John Turneaure, Physica C 212 (1993), 216-222.

[7] J. Pearl, Applied Physics Letters, Vol. 5, No. 4, 65 (1965).

[8] D. K. Finnemore, T. F. Stromberg, and C. A. Swenson, Phys. Rev. **149**, 231 (1966).

[9] Y. B. Kim, C.F. Hempstead, and A.R. Strnad, Phys. Rev. **129**, 528 (1962).

[10] D. J. Frankel, J. Appl. Phys. **50**,5402 (1979).

[11] L. W. Conner and A. P. Malozemoff, Phys. Rev. B. **43**, 402 (1991).

[12] William R. Smythe, *Static and Dynamic Electricity*, 2nd Edition (McGraw-Hill Book Company, Inc., 1950), pp. 325.

[13] Frederick W. Grover, *Inductance Calculations: Working Formula and Tables*, 2nd Edition (Dover Publications, Inc., 1962), pp. 143.

[14] J. Zhu, James Lockhart, and John Turneaure, Physica B **194**, 1357(1994).

Fig. 1. Experiment setup

The heaters and thermometers are used to control the sample temperature; the feedback current is inductively coupled to the SQUID input loop to cancel the stray coupling of the pickup loop.

Fig. 2. Magnetic hysteresis loops measured on sample #4 at 8.56K (T_c = 8.76K)

Left: the sample was FC in a field of +0.5 Oe; the initial magnetization curve crosses the equilibrium magnetization hysteresis loop. Right: the same sample was FC in a field of −0.5 Oe; the initial magnetization curve is higher than the later magnetic hysteresis loop. An ac field of $0.5\sin(2\pi ft)$ Oe was applied to measure the hysteresis loops, where $f = 10^{-3}$Hz.

Fig. 3. Magnetic hysteresis loops measured at 7.89K on sample #2 (T_c = 8.57K)

Left: ZFC sample. Right: the same sample was FC in a field of +2.4 Oe. The measurements were performed at a temperature well below the transition temperature. An ac field of $-1.2\sin(2\pi ft)$ Oe was applied to measure the hysteresis loops, where $f = 10^{-3}$Hz and the negative sign represents the initial condition.

Fig. 4. Calculated trapped flux density and current density

Top: trapped flux density versus radial position r, normalized to the disk radius R. Bottom: current density in the disk. Curves A and C appear to be nearly indistinguishable in the top part of the figure. Curves A, B, and C in this figure correspond to the points **A**, **B**, and **C** in Fig. 2.

Fig. 5. Maximum flux density at the pickup loop in $+z$ and $-z$ direction

The z-component of the magnetic flux generated by the trapped vortices was measured by the pickup loop when the applied ac field was at its maximum in the $+z$ and $-z$ directions, where $+z$ was defined as the positive direction. An ac field of $0.3\sin(2\pi ft)$ Oe was applied to measure the hysteresis loops, where $f = 10^{-3}$Hz. Solid lines are guides for the eye only.

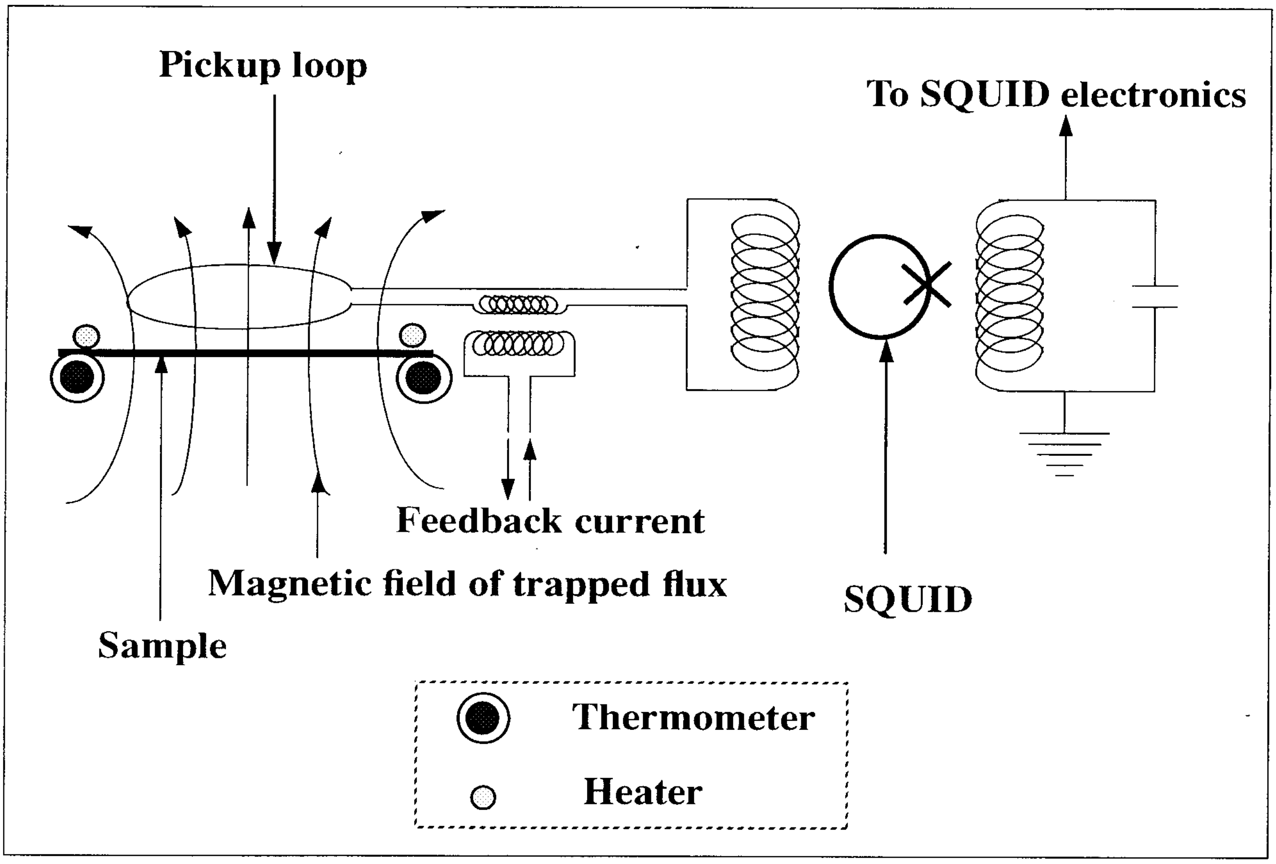
Pickup loop
To SQUID electronics
Feedback current
Magnetic field of trapped flux
SQUID
Sample
Thermometer
Heater

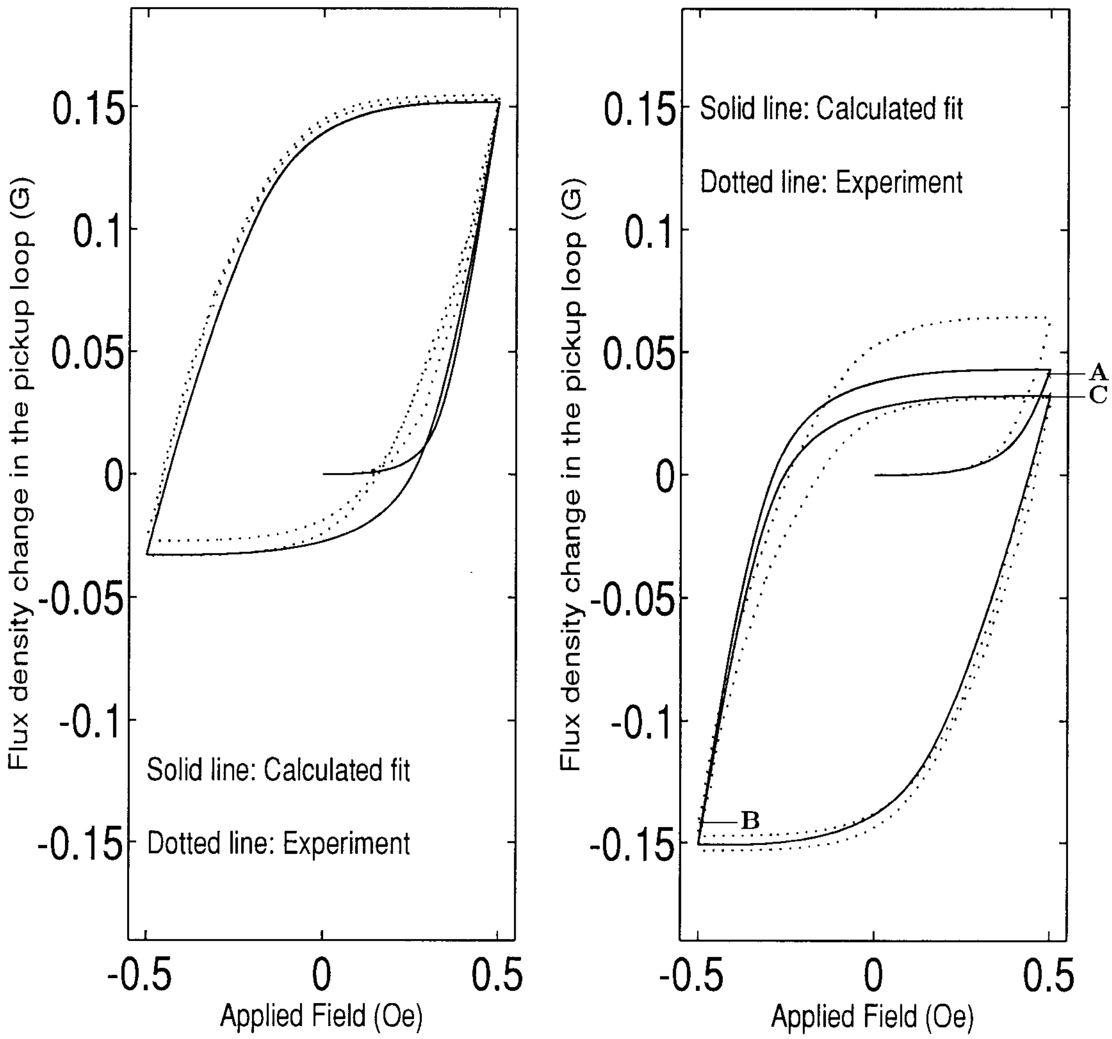
0.15
0.1
0.05
0
-0.05
-0.1
-0.15
Flux density change in the pickup loop (G)
Solid line: Calculated fit
Dotted line: Experiment
-0.5
0
0.5
Applied Field (Oe)
0.15
0.1
0.05
0
-0.05
-0.1
-0.15
Flux density change in the pickup loop (G)
Solid line: Calculated fit
Dotted line: Experiment
A
C
B
-0.5
0
0.5
Applied Field (Oe)

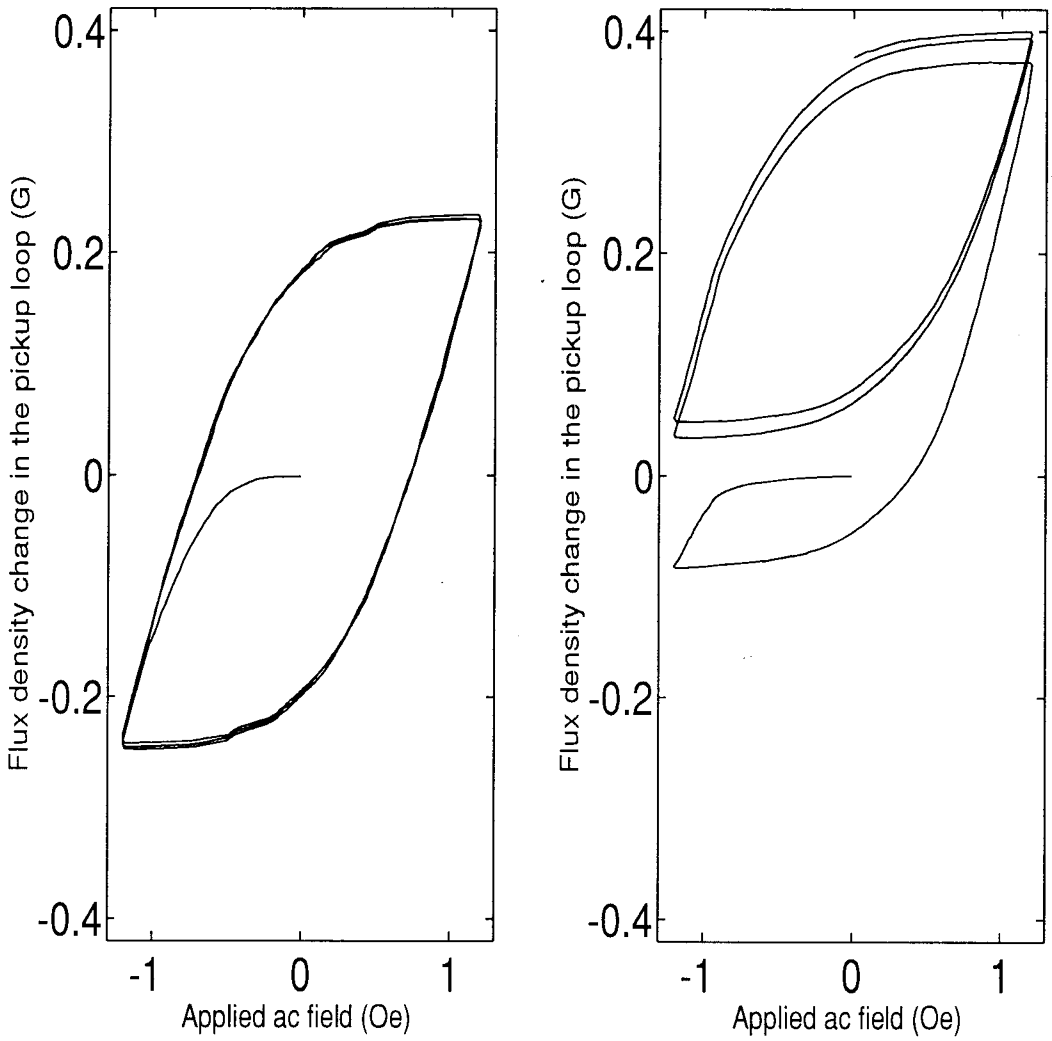

0.4
0.2
0
-0.2
-0.4
Flux density change in the pickup loop (G)
-1
0
1
Applied ac field (Oe)
0.4
0.2
0
-0.2
-0.4
Flux density change in the pickup loop (G)
-1
0
1
Applied ac field (Oe)

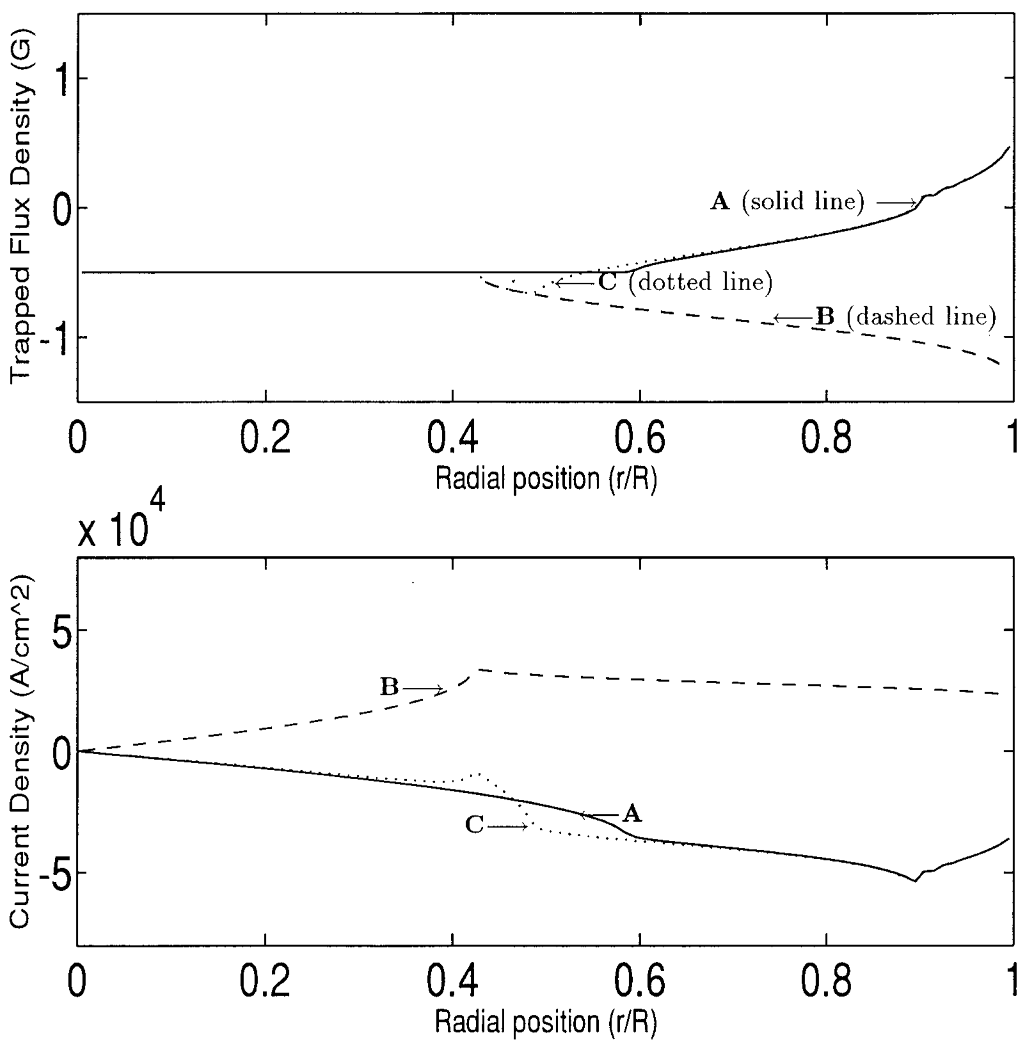

Trapped Flux Density (G)
1
0
-1
A (solid line)
C (dotted line)
B (dashed line)
0
0.2
0.4
0.6
0.8
1
Radial position (r/R)
x 10^4
Current Density (A/cm^2)
5
0
-5
B
A
C
0
0.2
0.4
0.6
0.8
1
Radial position (r/R)

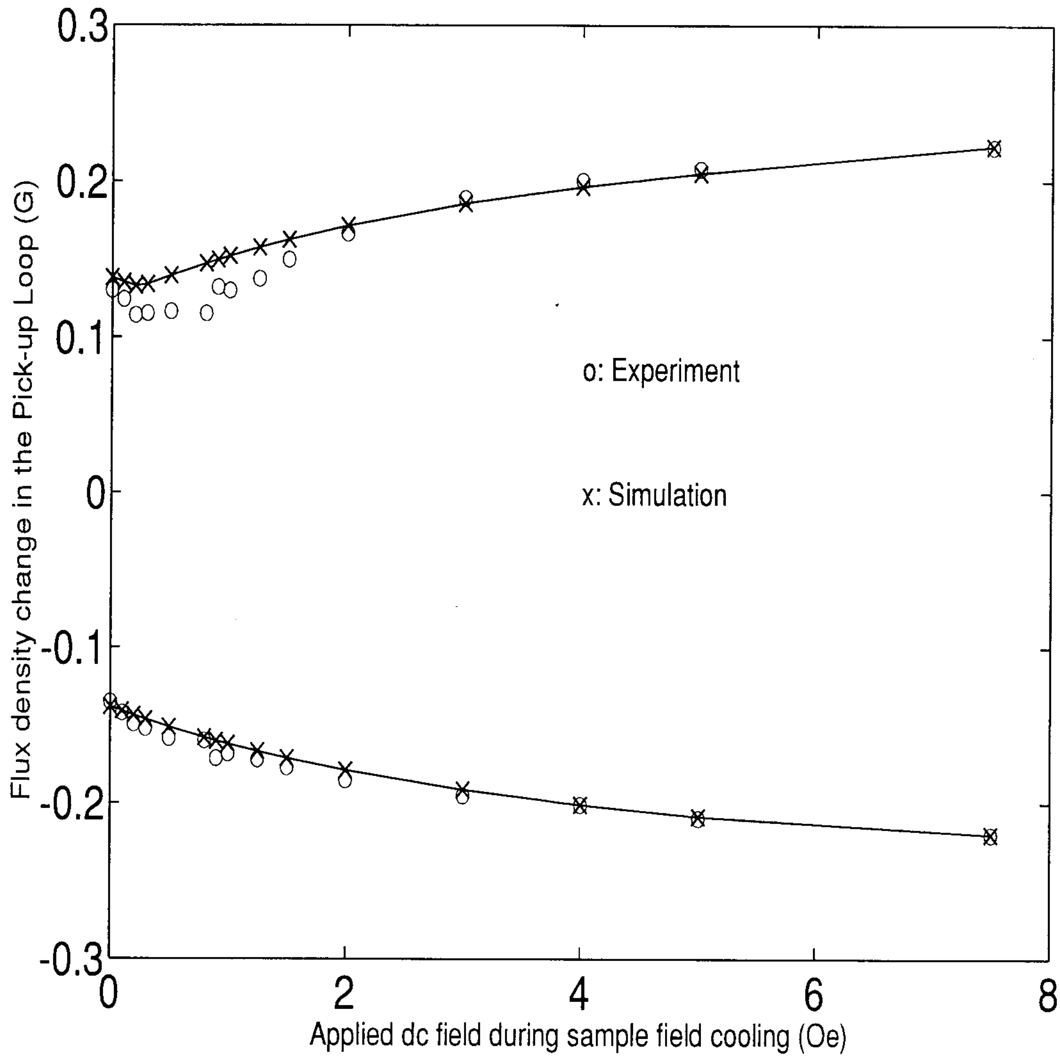
0.3
0.2
0.1
0
-0.1
-0.2
-0.3
Flux density change in the Pick-up Loop (G)
o: Experiment
x: Simulation
0
2
4
6
8
Applied dc field during sample field cooling (Oe)